Analytical dual-link MIMO channel model using correlated correlation matrices

Hult, Tommy; Tufvesson, Fredrik; Kolmonen, Veli-Matti; Poutanen, Juho; Haneda, Katsuyuki

2010

EUROPEAN COOPERATION
IN THE FIELD OF SCIENTIFIC
AND TECHNICAL RESEARCH

EURO-COST

COST 2100 TD(10) 10052
Athens, Greece
2010/Febr/3-5

SOURCE: 1. Department of Electrical and Information Technology,
Lund University,
Sweden
2. Department of Radio Science and Engineering,
School of Science and Technology,
Aalto University,
Finland

Analytical Dual-Link MIMO Channel Model using Correlated Correlation Matrices

1. Tommy Hult and Fredrik Tufvesson

2. Veli-Matti Kolmonen, Juho Poutanen and Katsuyuki Haneda

Tommy Hult
Department of Electrical and
Information Technology
Lund University
Box 118
SE-22100 Lund
SWEDEN
Phone: + 46-46-2224910
Fax: + 46-46-129948
Email: tommy.hult@eit.lth.se

Analytical Dual-Link MIMO Channel Model using Correlated Correlation Matrices

Tommy Hult[*], Fredrik Tufvesson[*], Veli-Matti Kolmonen[#], Juho Poutanen[#], Katsuyuki Haneda[#]

[*] *Dept. of Electrical and Information Technology, Lund University*
P.O. Box 118, SE-221 00 Lund, Sweden
{tommy.hult, fredrik.tufvesson}@.eit.lth.se

[#] *SMARAD CoE, Aalto University, School of Science and Technology, Finland*
{velimatti.kolmonen, katsuyuki.haneda}@.tkk.fi, jpoutane@cc.hut.fi

Abstract

Analytical Multiple-Input Multiple-Output (MIMO) models are often attractive due to their low complexity when analyzing possibilities and limitations in the system. In this paper we outline a a possible dual link extension of an analytical MIMO channel model and investigate its suitability based on measurements of a dual link MIMO scenario. The extension is based on the correlation matrix distance (CMD) as a gauge to generate correlation matrices for the additional links of the multi-link scenario.

1. Introduction

For the analysis and design of Multi-user Multiple-Input Multiple-Output (MIMO) systems it is helpful to have a simple but yet accurate analytical channel model that can capture the essential behavior of the radio channel. In MIMO systems the correlation properties is of special interest since it limits the performance and determines the effective degrees of freedom of the system. Several analytical models have been proposed for single link analysis. The simplest one is the so called Kronecker model [1]-[2], more accurate or versatile analytical models include, e.g., the full correlation model [3], the Weichselberger model [4] and the virtual channel representation [5]. Further, [6] presented a stochastic time-variant, frequency-selective, propagation-based single-link MIMO channel model.

In this paper we aim to extend the classical analytical MIMO correlation models to a multi-link scenario. We study both intra-link correlations, the "conventional" correlation matrix between the channel values belonging to one MIMO link, as well as inter-link correlations, loosely speaking the correlation of the intra-link correlation matrices, of a measured dual link MIMO scenario. Based on this we propose an analytical MIMO model using the correlation between the two intra-link correlation matrices as a gauge to generate correlation matrices for the two links in a dual-link scenario. Measurements show that the intra-link correlation of one link is correlated with the intra-link correlation of the other link, so there exist a inter correlation between the two correlation matrices, i.e. a non-zero correlation of the conventional correlation matrices. Similarly, the measurements have shown that two separate MIMO links may be affected by correlated shadow fading [10] even though they are quite far from each other.

2. Measurement Setup and Parameter Extraction

A. The Scenario

The measurement system consists of a dual-link wideband MIMO channel sounder operating at 5.3 GHz [12]. The transmitted power of the TX is 27 dBm (0.5 W) using a semi-spherical antenna array of 32 array elements. Receiver 1 (LU-RX) is using a cylindrical array of 32 array elements forming a 32 × 32 channel MIMO system together with the TX and receiver 2 (TKK-RX) is utilizing 30 array elements of a semi-spherical antenna array forming a 30 × 32 channel MIMO system with the TX.

We consider an indoor environment, see Fig.1, where the multi antenna transmitter (TX) is moving along a continuous route, shown in Fig.1, and the two multi antenna receivers (LU-RX and TKK-RX) are located at fixed positions. The measurement was carried out in the Computer Science Building at Helsinki University of Technology, TKK. The building is a typical modern office environment with a large hall in the middle of the building, surrounded by offices. A detailed description of the measurement system and the measurements can be found in [13]. The measurement scenario is deliberately chosen to include a medium high to high intra-correlation of the dual-link system, to provide a validation tool for the inter-link model. This follows from the observation that, if the intra-link correlation is low, there is no need to model the inter-link correlation as this one will also be low in the multipath-rich environment that typically results in low intra-link correlation.

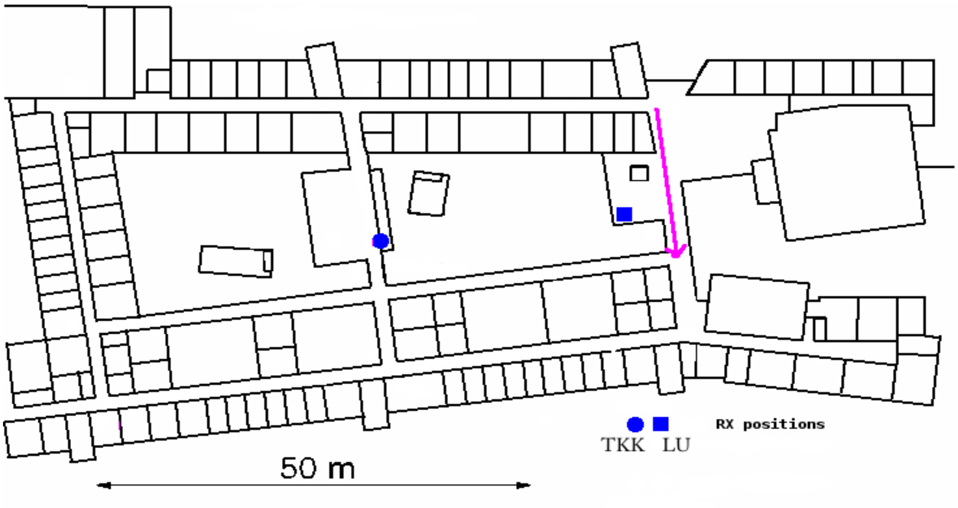

Figure 1. The measurement scenario, where the TX is following the route of the red arrow and the RX's are fixed in their positions (The blue circle and square markers).

B. Parameter Extraction

The parameters of the multipath components (MPCs) were estimated using the extended Kalman filter algorithm [8]. Based on these MPCs we generate complex valued channel matrices (transfer function matrices) for a 4 × 4 channel MIMO system using a simulated (virtual) four-element uniform linear array (ULA), with element spacing of half a wave length, at the receiver and transmitter respectively. Several independent realizations of channel matrices for each snapshot were generated using the experimental plane-wave based method [9] so that the phases of the different multipath components were altered similarly to [11]. This method provides $F=100$ frequency samples for each measured snapshot of the simulated four element uniform linear array.

After obtaining the 4 × 4 channel matrices for both links $\mathbf{H}_1(f,s)$ and $\mathbf{H}_2(f,s)$, the intra-correlation matrices were calculated. Here, three different intra-correlations can be used, the full correlation matrix, the correlation matrix at the transmitter and the correlation matrix at the receiver,

$$\mathbf{R}_{1,Full}(s) = N_r N_t \frac{\sum_{f=1}^{F} vec\{\mathbf{H}_1(f,s)\} vec\{\mathbf{H}_1(f,s)\}^H}{\sum_{f=1}^{F} \|\mathbf{H}_1(f,s)\|_F^2}, \quad (1)$$

$$\mathbf{R}_{1,TX}(s) = N_t \frac{\sum_{f=1}^{F} \mathbf{H}_1(f,s)^T \mathbf{H}_1(f,s)^*}{\sum_{f=1}^{F} \|\mathbf{H}_1(f,s)\|_F^2}, \quad (2)$$

$$\mathbf{R}_{1,RX}(s) = N_r \frac{\sum_{f=1}^{F} \mathbf{H}_1(f,s) \mathbf{H}_1(f,s)^H}{\sum_{f=1}^{F} \|\mathbf{H}_1(f,s)\|_F^2}. \quad (3)$$

where ^{H} denotes conjugate transpose and $\|\cdot\|_F$ is the Frobenius norm. For computational reasons we are, in this paper, only using the correlation at the TX in equation (2) and correlation at the RX in equation (3).

C. Measurement results

Fig. 2 shows the scatter plots of the RX and TX intra-link correlation matrix elements of the receivers and the transmitter. On the x-axis is the magnitude of the matrix elements of the first row of the RX or TX intra-correlation matrix for the first link (in this case LU-RX) is plotted against the corresponding matrix elements of the RX or TX intra-correlation matrix of the second link (TKK-RX).

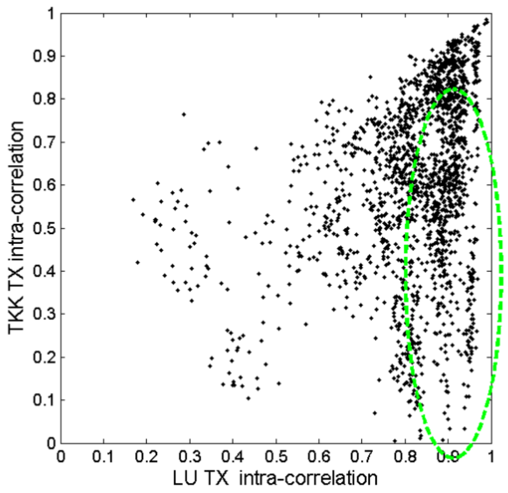

Figure 2. Scatter plot of the intra-link TX-correlation matrix elements of the two links.

The probability distributions of the channel magnitudes of the two links have some influence on the correlation between the links. The second link (TKK) has a reasonably constant "near Rayleigh" Ricean distribution with a K-value of ~ 0 – 0.9, while the first link (LU) is varying between a "near Rayleigh" and a clear Rice distribution with K-value of ~ 0.7 – 2.4.

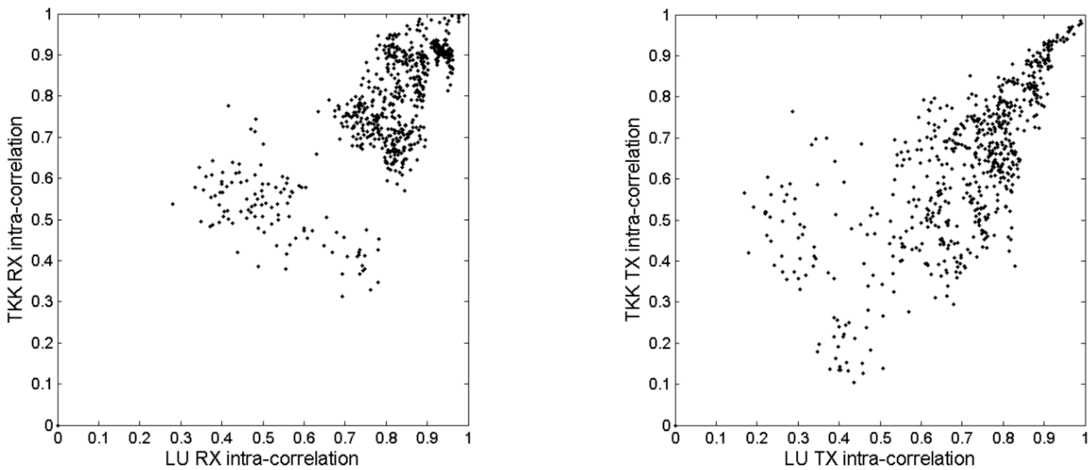

Figure 3. Scatter plots of the RX and TX intra-link correlation matrix elements of the two links, where the probability density functions of the amplitudes of the two links are similar.

In Fig. 2, the green ellipse shows roughly the correlation values where the probability distributions differ significantly which also give a low correlation between the two links.

In Fig. 3 we are only using those parts of the measurements were we have a similar probability distribution in both links with, in this case a Ricean K-value of ~ 0.5 – 1. From Fig. 3, where we have similar pdf's in the two links, it can clearly be seen that there is an inter-link correlation, especially at high correlation values. Therefore, when the LU correlation is high there is an increased probability that the TKK correlation will be high as well.

The correlation of correlation $\mathbf{R}'$ is calculated over the snapshots for which the correlation matrices were calculated using,

$$\mathbf{R}' = \frac{1}{S}\sum_{s=1}^{S} vec\left\{\left|\mathbf{R}_1(s)\right|\right\} \cdot vec\left\{\left|\mathbf{R}_2(s)\right|\right\}^H, \qquad (4)$$

where the structure of the correlation of correlation for the TX and RX side respectively, is plotted in Fig. 4. The correlation of correlation values varies between 1 and 0.6 for the TX and between 1 and 0.5 for the RX, which indicates that the inter-link correlation can be quite high. This suggests that the inter-link correlation cannot be neglected when modeling the dual-link behavior.

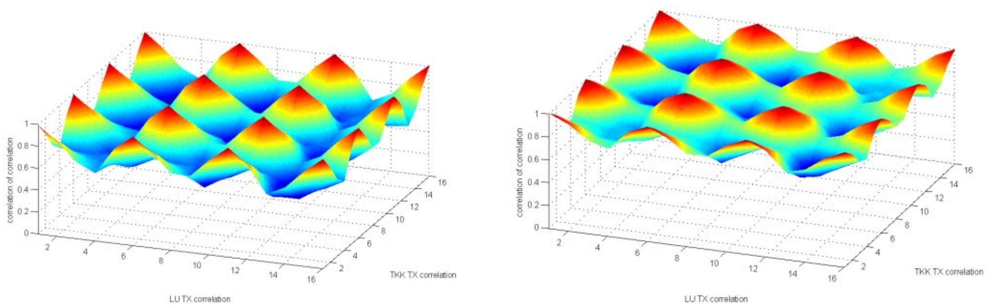

Figure 4. Elements in the correlation of correlation matrix for the TX side (left figure) and RX side (right figure).

3. Model Description

In order to model the dual-link MIMO channel we begin by defining the type of environment that the two links are experiencing. The environment (i.e., LOS or NLOS), in turn, determine the probability density function (PDF) of the stochastic processes for the two links. From the measurement results in Fig. 2 and Fig. 3 it is observed that both links require the same type of PDF for this link-correlation model to be valid.

For simplicity, we generate channel realizations by assuming a so called Kronecker model,

$$\mathbf{H} = \mathbf{R}_{\mathrm{RX}}^{1/2}\mathbf{H}_w\mathbf{R}_{\mathrm{TX}}^{1/2}, \qquad (5)$$

where $\mathbf{H}_{\mathrm{w}}$ is a spatially white identically independently distributed (i.i.d.) channel realization and $\mathbf{R}_{\mathrm{RX}}$ and $\mathbf{R}_{\mathrm{TX}}$ are the spatial intra-link correlations at the transmitter and receiver antenna arrays calculated in equations (2) and (3). Although, we consider the Kronecker case here, it is fairly straightforward to extend the model into, e.g., the full correlation model.

Measurements usually show that the intra-correlation matrices vary both with respect to the environment as well as the specific location of the transmitter and receiver. Some environments provide geometry with a narrow angular spread, which in turn results in large intra-correlation, whereas some environments provide a wider angular spread and a smaller spatial intra-correlation. Similarly, depending on the specific location of the transmitter or receiver, the line-of-sight component or other dominating components may be more or less visible at specific locations, creating a variation in the resulting correlation matrices.

To capture those variations we model the intra-correlation matrices of the two links as dependent random variables, with a certain mean and variance. The dependency is described by the inter-link correlation matrix, shown in Fig. 4 and by the co-linearity of the intra-correlation matrices of the two links. As a metric of the co-linearity we use the correlation matrix distance (CMD),

$$d_{R_1,R_2}(s) = 1 - \frac{\left|\mathrm{Tr}\left(\mathbf{R}_1(s)\mathbf{R}_2(s)\right)\right|}{\left\|\mathbf{R}_1(s)\right\|_F \cdot \left\|\mathbf{R}_2(s)\right\|_F}. \qquad (6)$$

Since the CMD can be reformulated as

$$\frac{\mathrm{Tr}\left(\mathbf{R}_1(s)\mathbf{R}_2(s)\right)}{\left\|\mathbf{R}_1(s)\right\|_F \left\|\mathbf{R}_2(s)\right\|_F} = \frac{vec\left\{\mathbf{R}_1(s)\right\}^H \cdot vec\left\{\mathbf{R}_2(s)\right\}}{\left\|vec\left\{\mathbf{R}_1(s)\right\}\right\|_2 \left\|vec\left\{\mathbf{R}_1(s)\right\}\right\|_2} = \overline{\mathbf{r}}_1 \cdot \overline{\mathbf{r}}_2 = \cos\left(\theta_{r_1 r_2}\right), \quad (7)$$

where $\overline{\mathbf{r}}_1$ and $\overline{\mathbf{r}}_2$ are the vectorized and normalized correlation matrices $\mathbf{R}_1$, $\mathbf{R}_2$ and $\theta_{r_1 r_2}$ can be seen as a rotation angle between the two correlation matrices $\mathbf{R}_1$ and $\mathbf{R}_2$. This can in turn be interpreted as a degree of orthogonality between the links. Therefore, by setting a specific value of the CMD we can, by using the spatial correlation matrix of the first link construct a spatial correlation matrix for the second link using a mixing equation,

$$\mathbf{R}_2(s) = \left(1-\sqrt{\gamma}\right)\mathbf{R}_1(s) + \sqrt{\gamma}\mathbf{R}_1^{\perp}(s), \quad (8)$$

where γ is the CMD value, $\mathbf{R}_1$ is the intra-correlation matrix of the first link and $\mathbf{R}_1^{\perp}$ is a matrix orthogonal to $\mathbf{R}_1$ generated by,

$$\mathbf{R}_1 = \begin{cases} \dfrac{\mathbf{H}\mathbf{H}^H}{\left\|\mathbf{H}\mathbf{H}^H\right\|_F}, & \text{on the RX side} \\ \dfrac{\mathbf{H}^T\mathbf{H}^*}{\left\|\mathbf{H}^T\mathbf{H}^*\right\|_F}, & \text{on the TX side} \end{cases}$$
$$\mathbf{R}_1^{\perp} \equiv \frac{\mathbf{R}_1^{-1}}{\left\|\mathbf{R}_1^{-1}\right\|_F} \quad (9)$$

where $\mathbf{H}$ is the simulated Ricean channel model of the first link,

$$\mathbf{H} = \sqrt{\frac{K}{K+1}}\mathbf{L} + \sqrt{\frac{1}{K+1}}\mathbf{H}_w,$$
$$\mathbf{H}_w \in \mathcal{CN}_{N_{RX},N_{TX}}\left(\mathbf{0}_{N_{RX}\times N_{TX}}, \mathbf{I}_{N_{RX}\times N_{TX}}\right), \quad (10)$$

and $\mathbf{L}$ is the LOS matrix with the condition that $\mathrm{Tr}\left\{\mathbf{L}\mathbf{L}^H\right\} = N_{RX} \cdot N_{TX}$.

4. Simulation results

To be able to compare the channel statistics obtained by simulated values to the ones from the measurements we simulate a similar system environment as the measurements performed in section 2.B.

To obtain the simulated channel values, we start by generating two temporally white Ricean 4×4 channels according to equation (10), both with the same K-factor, ~ 0.8 in this case. This is due to the condition that both links need to have a similar probability distribution function. Since we want a temporal behavior that is similar to the measurements, the temporal correlation is extracted from the measured first link (LU) and used to filter the simulated temporally white Ricean channels to obtain a similar temporal behavior of the simulated channels. Next, to acquire the spatial intra-correlation of the first link we calculate the TX and RX intra-correlations of each snapshot from the measured first link using equation (2) and (3). The intra-correlation are then applied to the simulated temporally correlated Ricean channels by using equation (5).

To generate the statistics of the simulated second link, spatial intra-correlation matrices for the second link are calculated by equation (8) using the knowledge of the CMD which represents the inter-correlation between the measured first and second links. The obtained intra-correlation matrices are then applied to the simulated temporally correlated ricean channels of the second link by using equation (5).

In Fig. 5 we show a scatterplot of both the measured (dots) and the simulated (rings) intra-correlation values, where we have plotted the separate correlation coefficients of the first row in the correlation matrix for all the snapshots. From Fig. 5 it can be seen that the simulated and measured correlation coefficients are quite different, but seems to have a similar statistic. In Fig. 6 the comparison between the eigenvalue distributions of the measured link 2 channel and the simulated link 2 channel.

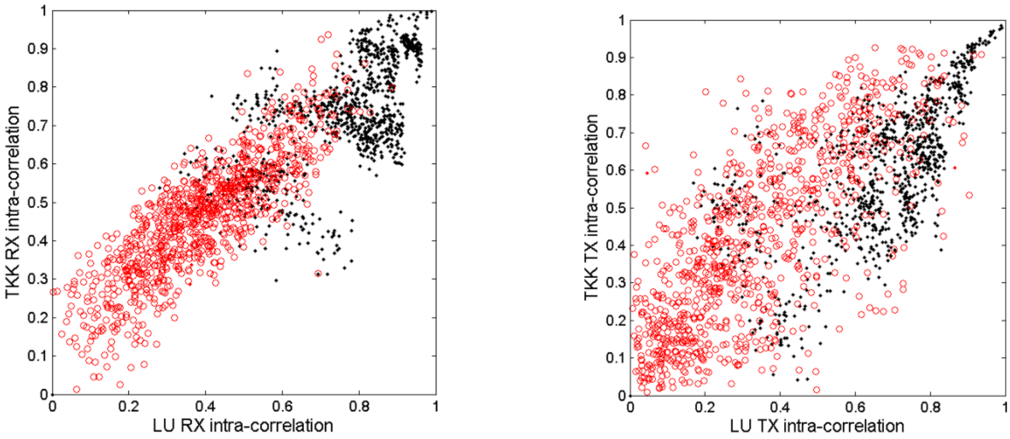

Figure 5. RX (top figure) and TX (bottom figure) Intra-correlation coefficients of Link 1 plotted against corresponding intra-correlation coefficients of Link 2 for the measured channel (dots) and for the simulated channel (rings).

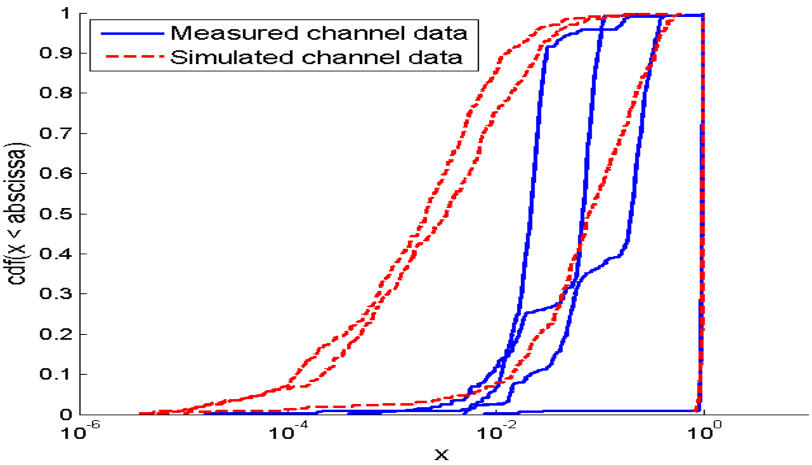

Figure 6. CDF of the four eigenvalue distributions for the measured and simulated link 2 channel.

Observing Fig. 6 it can be seen that the first and second eigenvalues have a fairly good match, while the two weaker values show more deviation. To see the effect of this eigenvalue deviation, the multipath richness [7] of the channel is plotted in Fig. 7 The richness value is calculated as the logarithm of the ratio between the geometric and arithmetic mean of the eigenvalues [7] to indicate how close the channel is to the i.i.d. channel,

$$richness = \log_2 \left(\frac{\left(\prod_{k=1}^{K} \lambda_k \right)^{1/K}}{\frac{1}{K} \sum_{k=1}^{K} \lambda_k} \right), \quad K = \min(N_t, N_r), \qquad (11)$$

where λ_k is the eigenvalue k, N_t and N_r is the number of transmitting and receiving antenna elements. A richness value of zero indicates an NLOS i.i.d. channel with uniform spatial distribution, while lower negative values indicate an LOS environment with some correlation between the channel values.

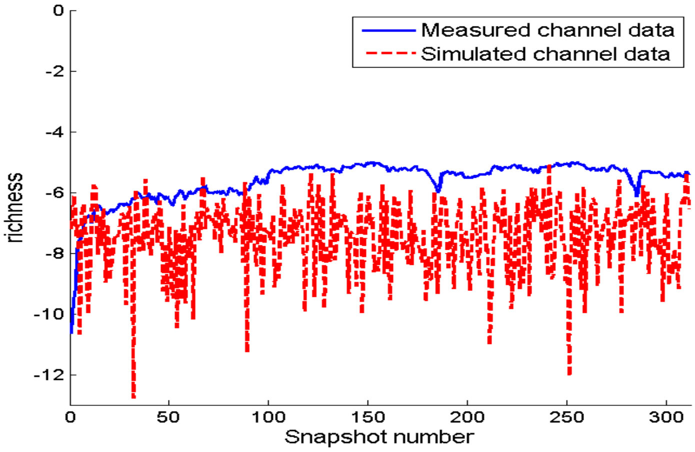

Figure 7. The richness value calculated for each snapshot of the measured and simulated channels.

From Fig. 7 we can observe that the simulated channel richness is lower than the measured channel richness, This is consistent with the eigenvalue distributions in Fig. 6, since the measured eigenvalues show a closer resemblance to an i.i.d. channel than the simulated channel due to the assumption that both links have the same temporal correlation.

5. Conclusions

From these preliminary results we have outlined a method for an analytical dual link MIMO channel model. It seems possible, provided that both links have similar probability distributions, to generate channel matrices for the dual link scenario that show both similar intra-link correlation and inter-link correlation.

To validate the model we used the *eigenvalue distribution,* and the *multipath richness*. The multipath richness shows a similar behavior for both the simulated values and for the directly measured values, apart from some deviations in the smaller eigenvalues. For future work, one should try using larger simulated arrays to obtain a better accuracy, also to investigate how much the pdf of the two links can deviate and also more measurement routes and scenarios should be investigated.

Acknowledgment

This paper has been written within the framework of WILATI+ which is a joint project between three Scandinavian universities and a part of the NORDITE research program funded by the Finnish, Swedish and Norwegian national research institutes Tekes, Vinnova and RCN, respectively.

References

[1] D. Shiu, G.J. Foshini, M.J. Gans and J.M. Khan, “Fading Correlation and its Effect on the Capacity of Multielement Antenna System”, *IEEE Transactions on Communications,* vol.48, no.3, pp.502-513, March 2000.

[2] J.P. Kermoal, L. Schumacher, K.I. Pedersen, P.E. Mogensen and F. Fredriksen, “A Stochastic MIMO Radio Channel Model with Experimental Validation”, *IEEE Journal on Selected Areas in Communications,* vol.20, no.6, pp.1211-1226, Augusti 2002.

[3] C. Oestges, “Validity of the Kronecker Model for MIMO Correlated Channel”, IEEE 63rd Vehicular Technology Conference, VTC 2006-Spring, vol.6, pp.2818-2822, 7-10 May, 2006.

[4] W. Weichselberger, M. Herdin, H. Özcelik, and E. Bonek, "A Stochastic MIMO Channel Model with joint Correlation of both Link Ends", *IEEE Transactions on Wireless Communications,* 2005.

[5] A.M. Sayeed, "Deconstructing Multiantenna Fading Channels", *IEEE Transactions on Signal Processing,* vol.50, no.10, pp.2563-2579, October 2002.

[6] N. Czink,T. Zemen, J-P. Nuutinen, J. Ylitalo and E. Bonek, "A Time-Variant MIMO Channel Model Directly Parametrised from Measurements", EURASIP Journal onWireless Communications and Networking, Vol. 2009, Article ID 687238, 2009.

[7] J. Salo, P. Suvikunnas, H. M. El-Sallabi and P. Vainikainen, "Ellipticity Statistic as a Measure of MIMO Multipath Richness," *Electronics Letters*, vol.42, no.3, pp. 45–46, Feb. 2006.

[8] J.Salmi, A. Richter, and V. Koivunen, "Detection and tracking of MIMO propagation path parameters using state-space approach," *IEEE Transactions on Signal Processing*, volume 57, number 4, pages 1538-1550, 2009.

[9] P. Suvikunnas, J.Villanen, K. Sulonen, C. Icheln, J.Ollikainen, and P. Vainikainen, "Evaluation of the Performance of Multiantenna Terminals Using a New Approach," *IEEE Transactions on Instrumentation and Measurement,* Vol. 55, No. 5, pp. 1804-1813, October 2006.

[10] J. Poutanen, K. Haneda, V.-M. Kolmonen, J. Salmi, and P. Vainikainen, "Analysis of Correlated Shadow Fading in Dual-Link Indoor Radio Wave Propagation", COST 2100 TD(09)910, Vienna, Austria, 28-30 September, 2009.

[11] Molisch, A.F.; Steinbauer, M.; Toeltsch, M.; Bonek, E.; Thoma, R.S., "Capacity of MIMO systems based on measured wireless channels ", *IEEE Journal on Selected Areas in Communications*, Vol. 20, no.3, pp. 561-569, 2002.

[12] J. Koivunen, P. Almers, V.-M. Kolmonen, J. Salmi, A. Richter, F. Tufvesson, P. Suvikunnas, A.F. Molisch, and P. Vainikainen, "Dynamic multi-link indoor MIMO measurements at 5.3 GHz," in Proc. 2nd European Conference on Antennas and Propagation 2007, (EuCAP 2007), Edinburgh, UK, Nov. 2007.

[13] V.-M. Kolmonen, P. Almers, J. Salmi, J. Koivunen, K. Haneda, A. Richter, F. Tufvesson, A. F. Molisch, and P. Vainikainen "A dynamic dual-link wideband MIMO measurement system for 5.3 GHz," accepted for publication in IEEE Trans on Instrumentations and Measurement, 2009.